Sādhanā (2018) 43:46
https://doi.org/10.1007/s12046-018-0838-6

Assessment of the toughness of fibre-reinforced concrete using the R-curve approach

STEFIE J STEPHEN[1,*], RAVINDRA GETTU[1], LUIZ EDUARDO TEIXEIRA FERREIRA[2] and SUJATHA JOSE[1]

[1]Department of Civil Engineering, Indian Institute of Technology Madras, Chennai 600036, India
[2]Department of Engineering, Federal University of Lavras, Lavras, MG 37200-000, Brazil
e-mail: stefie.j.s@gmail.com; gettu@iitm.ac.in; luizeduardo.ferreira@deg.ufla.com

MS received 30 January 2017; revised 9 July 2017; accepted 12 March 2018; published online 28 March 2018

Abstract. The fracture response of brittle materials like concrete can be characterised using modified linear elastic fracture mechanics models, such as the rising resistance curve (R-curve). In this study, the R-curve, determined by utilising the experimental response in the notched beam test with mode I fracture, is proposed as a measure of the toughness of fibre-reinforced concretes (FRCs). The unambiguity of the R-curve obtained is assessed by comparing the predicted flexural response of specimens of different geometries with experimental data. The variation in the R-curves with the dosage of steel and polymer fibres is also discussed.

Keywords. R-curve; linear elastic fracture mechanics; mode I fracture; notched beam test; flexural toughness; fibre-reinforced concrete.

1. Introduction

Fibres are added in concrete to improve the toughness and energy absorption capacity [1]. The crack-bridging ability of fibres in the concrete facilitates applications in pavements, slab-on-grade, tunnel linings, bridge decks, etc. As the fibre effectiveness and concentration increase, crack propagation is prevented and the concrete toughness increased [2]. Four- and three-point bendings are the commonly used testing configurations, from which toughness parameters, such as equivalent and residual strength, are obtained based on simple elastic bending theory at the crack plane [3–7]. For instance, the residual strength of fibre-reinforced concrete (FRC) at a specific deflection, for example, serviceability limit (0.5 mm), is calculated considering the whole depth of the beam, ignoring any crack growth.

Approaches based on the rising resistance curve (R-curve) have been used to represent the evolution of fracture and the improved toughness due to the incorporation of fibres in concrete [8–11]. It has been shown that in a body of infinite size, where the full fracture process zone can be developed in an unhindered manner [12–14], the R-curve reaches a plateau. However, in a smaller specimen, the R-curve keeps rising, thus making it dependent on specimen size and geometry [15–18], especially at the unstable fracture [19–23]. The significance of the R-curve is that, in spite of the curve being dependent on geometry and material, the constitutive relation of the material appear to be correlated [24]. Recently, Mobasher *et al* [25] used the R-curve to determine the tensile stress–strain behaviour of FRC for use in the analysis of structural behaviour.

In the current work, data from three-point bending tests on notched FRC beams performed under crack mouth opening displacement control, following EN 14651 [6], are used to obtain the R-curves for steel and polymer FRC. The crack growth at different levels of loading is examined and the crack mitigation process of fibres is explained using the curve. The derived R-curve is later used to predict the flexural response of different geometries in order to assess the general applicability.

2. Fracture analysis

2.1 *Equations based on linear elastic analysis*

Though linear elastic fracture mechanics (LEFM) cannot be used for representing the behaviour of concrete, equations derived on the basis of this theory are needed for nonlinear fracture mechanics approaches such as the R-curve considered in this work. Further, there are geometry-dependent constants that have to be obtained using LEFM.

The flexural toughness testing of notched beam conforming to RILEM TC 162 Recommendation [5] and the EN 14651 standard [6] uses a centre-point loaded (P) beam with length (L) = 700 mm, width (b) = 150 mm, depth

*For correspondence

(d) = 150 mm, notch length (a_0) = 25 mm and span (l) = 500 mm (figure 1). The stress intensity factor for mode I fracture (K_I) in such a specimen with a relative crack length x can be expressed as

$$K_I = \frac{3Pl\sqrt{\pi a}}{2bd^2} f_I(x) \quad (1)$$

Similarly, the crack mouth opening displacement (CMOD) is given by

$$CMOD = \frac{6Pla}{Ebd^2} V_1(x) \quad (2)$$

where $f_I(x)$ and $V_I(x)$ are the dimensionless geometry-dependent LEFM functions, which can be determined by linear elastic analysis.

For the geometry considered in EN 14651, appropriate geometry-dependent functions have been determined using finite element analysis [26–28]:

$$f_I(x) = 0.4 + 7.3x - 41.6x^2 + 118.5x^3 - 156.3x^4 + 85.2x^5 \text{ for } 0.17 \le x \le 0.65 \quad (3a)$$

$$f_I(x) = \frac{0.604 - 0.547x}{1 - 2.026x + 1.027x^2} \quad \text{for } x > 0.65 \quad (3b)$$

$$V_1(x) = 0.197 + 17.816x - 107.63x^2 + 338.21x^3 - 494.26x^4 + 298.86x^5 \quad \text{for } 0.175 \le x \le 0.65 \quad (4a)$$

$$V_1(x) = \frac{0.817 - 0.218x}{1 - 2.011x + 1.012x^2} \quad \text{for } x > 0.65 \quad (4b)$$

2.2 *The R-curve*

The R-curve approach modifies LEFM by considering a varying critical stress intensity factor or fracture energy to account for the formation and progression of the fracture process zone. The R-curve is considered here as the relation between the critical stress intensity factor (K_{IR}) and the crack extension $\Delta a = a - a_0$, where a is the total crack length and a_0 is the initial notch length and denoted as $K_{IR}(\Delta a)$. The slope of the initial linear part of experimentally obtained load–CMOD curve can be used to determine the Young's modulus of the concrete, E, using the following equation derived from Eq. (2):

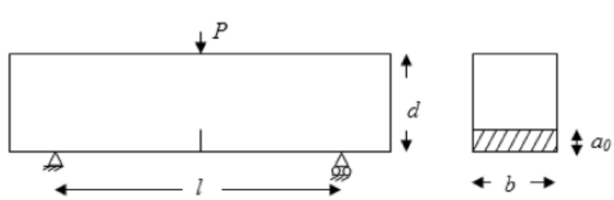

Figure 1. Test arrangement of a three-point notched beam specimen.

$$E = \frac{6Pla_0}{CMOD\ bd^2} V_1(x_0) \quad (5)$$

Table 1. Characteristics of the fibres used (as given by the manufacturer).

Properties	Steel fibres	Polymer fibres
Specific gravity	7.8	0.92
Length (mm)	60	40
Aspect ratio (length/diameter)	80	90
Characteristic tensile strength (MPa)	1225	620

Table 2. Fibre volume fraction and specimen notation.

Steel fibre dosage (kg/m^3); volume fraction	Specimen notation	Polymer fibre dosage (kg/m^3); volume fraction	Specimen notation
0; 0%	M40SF0	0; 0%	M40PF0
10; 0.1%	M40SF10	2.5; 0.3%	M40PF2.5
15; 0.2%	M40SF15	3.75; 0.4%	M40PF3.75
20; 0.3%	M40SF20	5; 0.54%	M40PF5
30; 0.4%	M40SF30		
45; 0.6%	M40SF45		

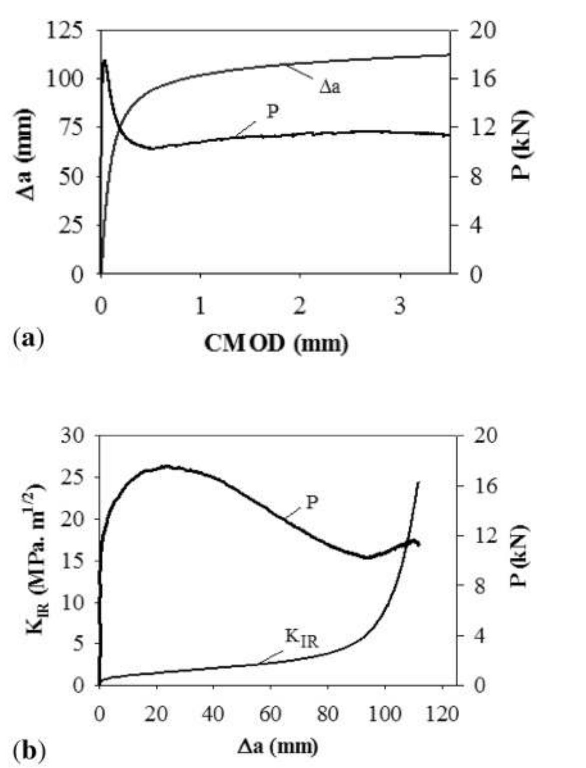

Figure 2. (**a**) Effective crack growth obtained from P-CMOD data and (**b**) the R-curve for fibre-reinforced concrete M40SF20.

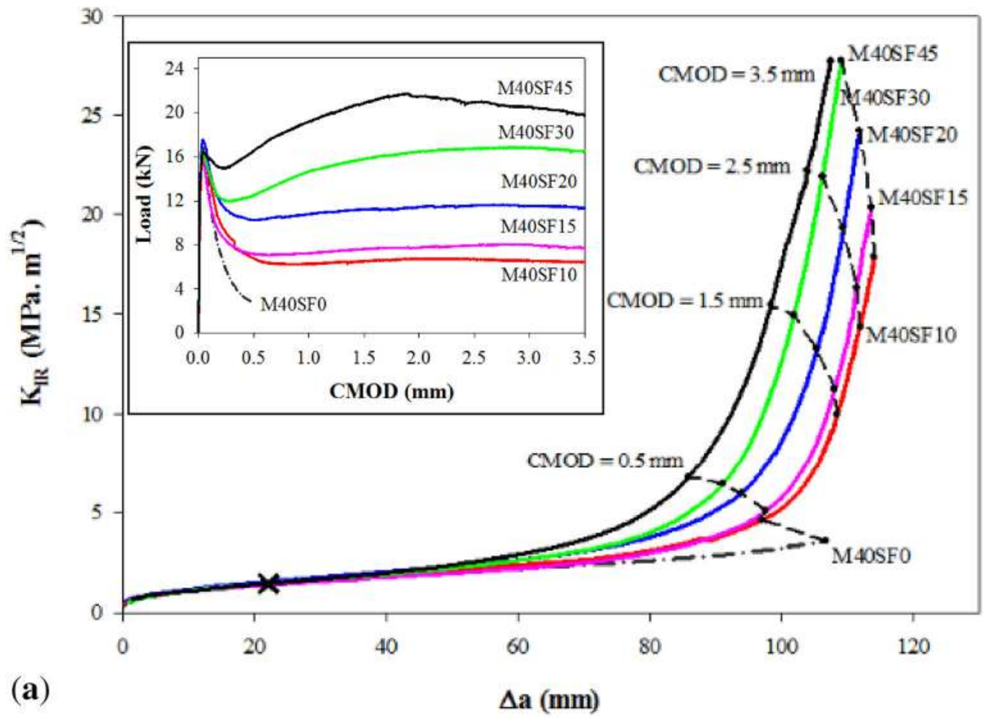

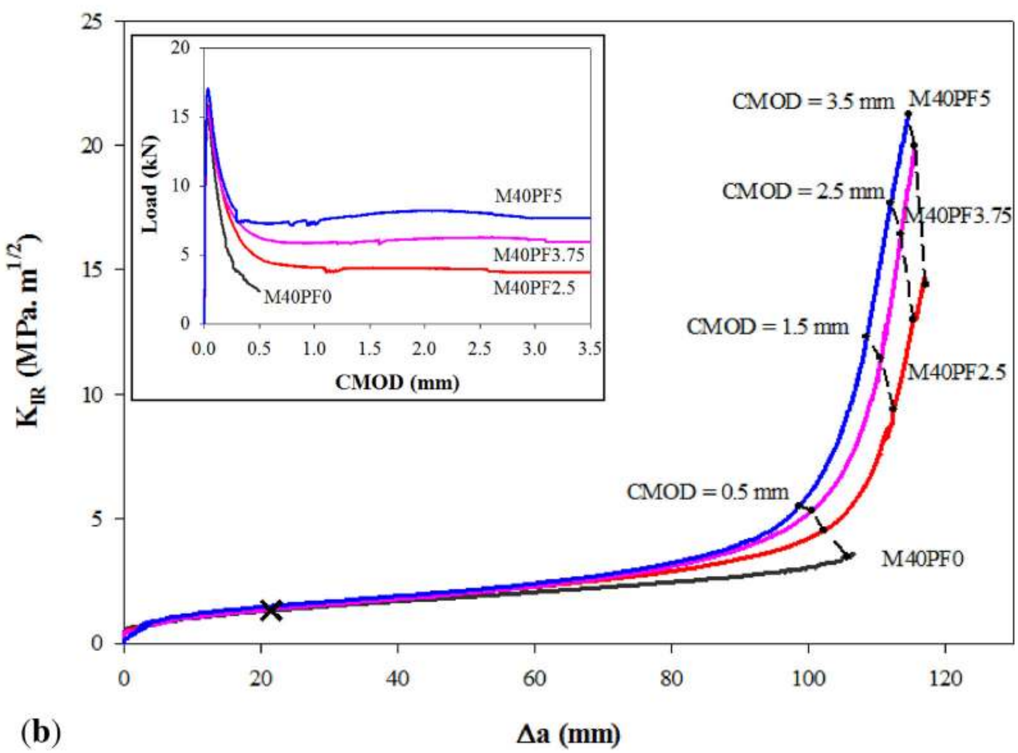

Figure 3. Comparison of crack resistance curves of concrete with different dosages of (**a**) steel fibres and (**b**) polymer fibres (insets show the experimental P-CMOD curves).

The relative crack length is obtained by iterating for x in the following equation after incorporating the secant compliance at different loads [17, 21, 29–31]:

$$\beta(x) = \frac{CMOD\ bdE}{6Pl} = xV_1(x) \qquad (6)$$

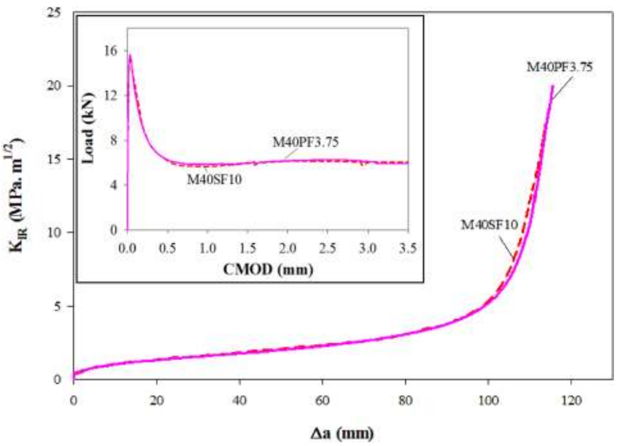

Figure 4. Similar R-curves for two different concretes with similar flexural response.

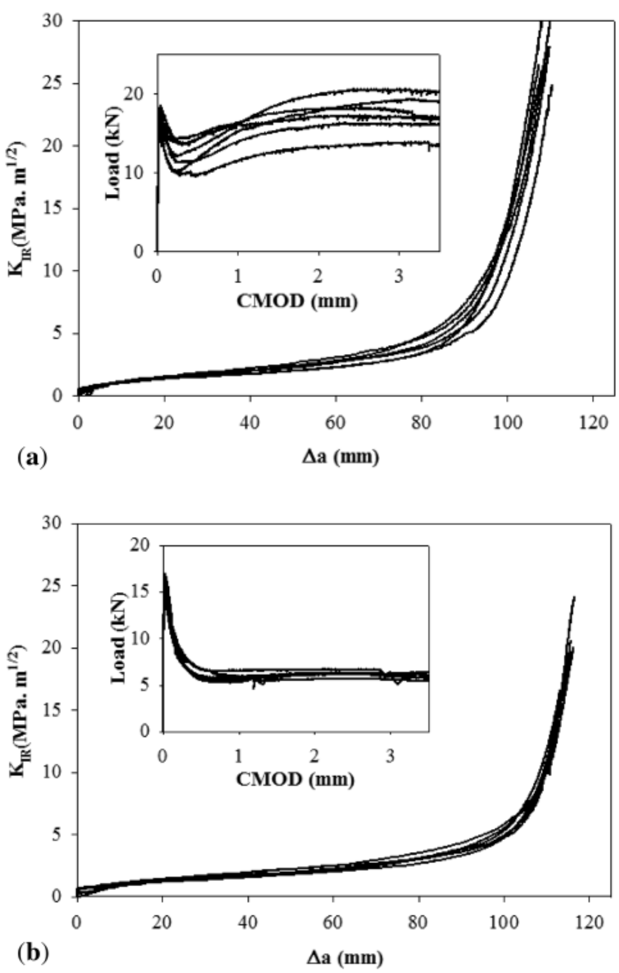

Figure 5. Variations in R-curves for concrete within the same set; (**a**) M40SF30 and (**b**) M40PF3.75 (the insets show the corresponding P-CMOD curves).

For different effective crack lengths, K_{IR} is calculated using Eq. (1) and Eq. (3a) or (3b), considering that the load–CMOD curve is governed by the propagating crack.

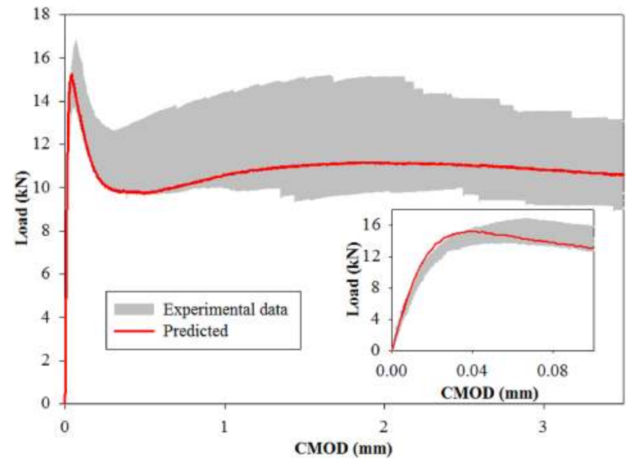

Figure 6. Flexural response of beam with notch length of 30 mm.

3. Application to fibre-reinforced concrete

Conventional M40 grade concrete (having a maximum aggregate size of 20 mm) with steel and polymer fibres is used for the assessment of toughness; six specimens were tested in each case. Table 1 presents the characteristics of the fibres used in the FRC. Hooked-ended cold-drawn steel fibres and polypropylene fibres have been used at different dosages (table 2).

For illustrating the methodology used for deriving the R-curve for a certain material, a beam specimen, with a notch length of 25 mm, made of concrete with steel fibres at the dosage of 20 kg/m^3 (M40SF20) is used. The variation of effective crack growth (Δa) obtained as a function of the CMOD, determined using Eq. (6), is shown in figure 2a, along with the experimentally obtained P-CMOD curve used in the derivation. A rapid change is seen in the crack growth until a CMOD value of about 0.5 mm, and the effective crack length is about 110 mm when the CMOD reaches 1.5 mm, beyond which there is no significant crack growth. The effective crack length and the corresponding experimental load are substituted in Eq. (1) to obtain the K_{IR}-value, the evolution of which is shown in figure 2b, along with the parent P-Δa curve. It is evident that stress intensity factor increases with an increase in crack length, as expected, and continues to do so even more rapidly when the crack propagation is constrained by the boundary of the specimen.

Typical R-curves for different dosages of steel fibres are shown in figure 3a, corresponding to the P-CMOD curves shown in the insets. The increase in toughness due to higher fibre dosage, reflected by a gradual change from softening to plastic-type response, leads to R-curves that are higher, especially beyond the peak load (indicated by the × in the plots, which does not change significantly with the fibre dosage) that occurs around the CMOD of 0.5 mm. The dashed lines in the graph indicate the effective crack length

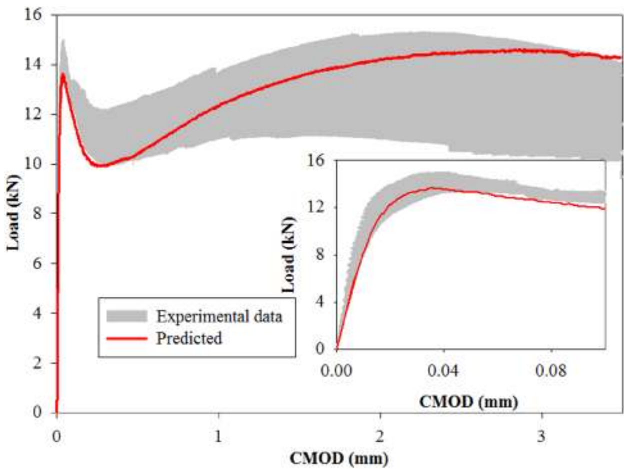

Figure 7. Flexural response of beam with span length of 600 mm.

for the various concretes at different CMOD levels. It can be observed that the crack growth at a particular CMOD is lower for concrete with higher dosage of fibres, which reflects the mitigation of crack progression by the fibres. Similar behaviour is observed in the polymer FRCs (figure 3b), except that the K_{IR}-values are lower than those of steel FRC, for the same volume fraction. This explains the lesser degree of toughening generally obtained in polymer FRCs than in steel FRCs, even though the fibre volume fractions are the same. However, if the P-CMOD curves are similar, for example, in the case of M40SF10 and M40PF3.75, the R-curves obtained are comparable, as expected; see figure 4.

The variation among R-curves within a certain set of FRC specimens, with same fibre type and volume fraction, is generally seen to be low, with the concretes reinforced with steel fibres exhibiting slightly more scatter than polymer fibres (as can be seen in figure 5). This is in accordance with previous studies that have attributed the lower scatter in polymer FRC response to the larger number of fibres present in a unit volume of concrete or across a crack face than in steel fibre concrete for the same volume fraction [2].

4. Prediction of P-CMOD curves using the R-curve

To assess whether the R-curve described earlier could be used to simulate the fracture response of specimens/elements different from that used to derive it, tests were performed on M40SF30 concrete specimens that are similar to those referred to earlier but with a different notch length or span.

The average R-curve obtained, from six tests on M40SF30 beams with notch length of 25 mm, was used to predict the response of a beam with a notch length of 30 mm using the LEFM functions already given in Eqs. (3) and (4). The predicted P-CMOD curve is compared with experimental data for this specimen geometry in figure 6, and is found to fall within the band of results though closer to the lower bound. This may be because of the slightly shorter crack extension in this case compared to the shorter notch length due to the boundary effect. It appears that the longer notch length results in the crack reaching the specimen boundary at a smaller CMOD than in the standard beam.

Similarly, the prediction was made for beams with a span length of 600 mm and notch length of 25 mm using the following LEFM equations derived for this purpose:

$$f_I(x) = 1.03 - 0.57x - 1.38x^2 + 20.87x^3 - 43.31x^4 + 34.96x^5 \quad \text{for } 0.17 \le x \le 0.65 \tag{7a}$$

$$f_I(x) = \frac{0.59 - 0.50x}{1 - 1.98x + 0.98x^2} \quad \text{for } x > 0.65 \tag{7b}$$

$$V_1(x) = 1.28 + 2.14x - 21.07x^2 + 113.32x^3 - 216.76x^4 + 168.06x^5 \quad \text{for } 0.17 \le x \le 0.65 \tag{8a}$$

$$V_1(x) = \frac{0.84 - 0.25x}{1 - 2.013x + 1.014x^2} \quad \text{for } x > 0.65 \tag{8b}$$

It can be seen in figure 7 that the prediction is within the experimental band of results, though the tail of the post-peak region approaches the upper bound. This may be attributed to the effect of the boundary in limiting crack growth beyond a crack opening of about 1.5 mm. This suggests that using the flexural response until a crack opening of 1.5 mm, beyond which the fracture does not propagate significantly, could give a more representative characterisation of the material behaviour instead of using the response until the CMOD of 3 or 4 mm.

5. Conclusions

The rising resistance curve (R-curve) obtained using the response of the FRC beam specimen tested in accordance with RILEM 162 TDF and EN14651 recommendations has been presented, and the following conclusions can be drawn from the study:

- The toughening effect of the fibres is well reflected by the R-curves obtained for concretes with different dosages of steel and polymer fibres.
- The K_{IR}-values are consistently higher for concretes with steel fibres than with polymer fibres for the same volume fractions.
- The R-curves obtained using the EN 14651 has been used satisfactorily to predict the flexural response for two other geometries.

- Since the crack progression beyond a crack opening of about 1.5 mm in the EN 14651 specimen is limited by the specimen boundary, it is proposed that toughness characterisation be limited to the crack width of 1.5 mm, instead of 3.5 mm. This is expected to provide more representative material characterisation without much effect of the specimen dimensions.

References

[1] Gopalaratnam V S and Gettu R 1995 On the characterization of flexural toughness in fibre reinforced concretes. *Cem. Concr. Compos.* 17(3): 239–254

[2] Nayar S K, Gettu R and Krishnan S 2014 Characterisation of the toughness of fibre reinforced concrete – revisited in the Indian context. *Indian Concr. J.* 88(2): 8–23

[3] ASTM C1609/C1609M-10 2010 Standard Test Method for Flexural Performance of Fiber Reinforced Concrete (Using Beam with Third-Point Loading), American Society of Testing and Materials, USA

[4] JSCE Part III-2 (SF1–SF4) 1984 *Method of Tests for Steel Fiber Reinforced Concrete.* Concrete Library of JSCE, Japan Society of Civil Engineers

[5] RILEM TC 162-TDF 2002 Test and design methods for steel fibre reinforced concrete: Bending test – Final recommendation. *Mater Struct.* 35(9): 579–582

[6] EN 14651 2005 *Test method for metallic fibered concrete – measuring the flexural tensile strength (limit of proportionality (LOP), residual)*, British Standards Institution

[7] ICI-TC/01.1 2014 Test methods for the flexural strength and toughness parameters of fiber reinforced concrete, Indian concrete institute technical committee recommendation. *Indian Concr. Inst. J.* 15(2): 39–43

[8] Ouyang C, Mobasher B and Shah S P 1990 An R-curve approach for fracture of quasi-brittle materials. *Eng. Fract. Mech.* 37(4): 901–913

[9] Eissa A and Batson G 1996 Model for predicting the fracture process zone and r-curve for high strength FRC. *Cem. Concr. Compos.* 18(2): 125–133

[10] Mobasher B and Li C Y 1996 Mechanical properties of hybrid cement-based composites. *ACI Mater. J.* 93: 284–292

[11] Dey V, Kachala R, Bonakdar A and Mobasher B 2015 Mechanical properties of micro and sub-micron wollastonite fibers in cementitious composites. *Constr. Build. Mater.* 82: 351–359

[12] Gettu R, Bažant Z P and Karr M E 1990 Fracture properties and brittleness of high-strength concrete. *ACI Mater. J.* 87(6): 608–618

[13] Bažant Z P, Gettu R and Kazemi M T 1991 Identification of nonlinear fracture properties from size effect tests and structural analysis based on geometry-dependent R-curves. *Int. J. Rock Mech. Min. Sci.* 28(1): 43–51

[14] Karihaloo B L 1995 *Fracture mechanics and structural concrete.* 1st edition, Longman Scientific and Technical, UK

[15] Foote R M L, Mai Y-W and Cotterell B 1986 Crack growth resistance curves in strain-softening materials. *J. Mech. Phys. Solids.* 34(6): 593–607

[16] Cotterell B and Mai Y-W 1987 Crack growth resistance curve and size effect in the fracture of cement paste. *J. Mater. Sci.* 22(8): 2734–2738

[17] Banthia N and Sheng J 1996 Fracture toughness of micro-fiber reinforced cement composites. *Cem. Concr. Compos.* 18(4): 251–269

[18] Mai Y W 2002 Cohesive zone and crack-resistance (R)-curve of cementitious materials and their fibre-reinforced composites. *Eng. Fract. Mech.* 69(2): 219–234

[19] Wecharatana M and Shah S P 1983 Predictions of nonlinear fracture process zone in concrete. *ASCE: J Eng. Mech.* 109(5): 1231–1246

[20] Bažant Z P, Kim J K and Pfeiffer P A 1986 Nonlinear fracture properties from size effect tests. *J Struct. Eng.* 112(2): 289–307

[21] Kumar S and Barai S V 2010 Determining the double-K fracture parameters for three-point bending notched concrete beams using weight function. *Fatigue Fract. Eng. Mater. Struct. 33*(10): 645–660

[22] Brake N A 2012 *The characterization of a plain concrete equivalent elastic fatigue crack resistance curve under various loading regimes*, Doctoral Thesis, Michigan State University, Michigan, USA

[23] Zhao Y, Chang J and Gao H 2015 A three-parameter R-curve of concrete-like quasi-brittle materials. *Constr. Build. Mater.* 78: 243–249

[24] Morel S, Lespine C, Coureau J, Planas J and Dourado N 2010 Bilinear softening parameters and equivalent LEFM R-curve in quasibrittle failure. *Int. J Solids. Struct.* 47(6): 837–850

[25] Mobasher B, Bonakdar A and Bakhshi M 2015 Back-calculation procedure for cyclic flexural fracture tests in fiber reinforced concrete. *Special Publication ACI J.* 300: 1–22

[26] García-Álvarez V O 1997 *Study of mixed mode fracture in quasi-brittle materials* (in Spanish). Doctoral Thesis, Universitat Politècnica de Catalunya, Barcelona, Spain

[27] Ferreira L E T, Bittencourt T N, Sousa J L A O and Gettu R 2002 R-curve behavior in notched beam tests of rocks. *Eng. Fract. Mech.* 69(17): 1845–1852

[28] García-Álvarez V O, Gettu R and Carol I 2017 Determination of the energy release rate function for an eccentrically notched center-loaded beam using elastic fracture analysis. *J. Struct. Eng.* 44(1): 88–94

[29] Xu S and Reinhardt H W 1998 Crack extension resistance and fracture properties of quasi-brittle softening materials like concrete based on the complete process of fracture. *Int. J. Fract.* 92(1): 71–99

[30] Wu Z, Yang S, Hu X and Zheng J 2006 An analytical model to predict the effective fracture toughness of concrete for three-point bending notched beams. *Eng. Fract. Mech.* 73(15): 2166–2191

[31] Wallin K 2013 A simple fracture mechanical interpretation of size effects in concrete fracture toughness tests. *Eng. Fract. Mech.* 99: 18–29